Proceedings World Geothermal Congress 2026
Calgary, Canada, June 8 – 11, 2026

Mayotte, Comoros Islands: A New Conceptual Model Of The Geothermal System Based On The Feedback Of The 2018-2020 Seismic And Submarine Volcanic Crisis.

Tchang-Tchong L.[1]*, Paquez C.[2], Traineau H.[1], Hautot S.[3] and Hirsinger L.[1]
CFG GEOTHERMAL[1]*, 45064 Orléans, FRANCE; ALBIOMA[2], La Défense, 92914 Puteaux, FRANCE; IMAGIR[3], 29290 Saint Renan, FRANCE
*l.tchang-tchong@cfg-geo.fr

Keywords: Mayotte, Comoros, geothermal resources, reservoir conceptual model, submarine deep reservoir, magnetotellurics, 3D resistivity model, gas emissions.

ABSTRACT

Mayotte island is part of the Comoros Archipelago in the Indian Ocean. Late Pleistocene volcanic activity led to the formation of two phonolitic maars above the coral reef, which subsequently formed a small island named Petite-Terre. Prominent gas emissions are observed for a long time in Petite-Terre, but no thermal springs. In 2018-2020, a seismic crisis and a submarine eruption revealed a submarine volcanic chain, with an important volcanic center located about 10 km ESE of Petite-Terre. Based on abundant geological, geochemical, geophysical and bathymetric data collected during the crisis, a new conceptual model of the geothermal system is proposed. It links the gas emissions observed on land to a nearby submarine volcanic center and a deep geothermal reservoir, where downward seawater infiltrations mix with upward high-temperature fluids from underlying magmatic chambers. Gas geothermometers suggest temperature of 250-300°C at depth. Magnetotelluric surveys on Petite-Terre Island reveal a resistivity pattern which is consistent with a 500-m-thick reef limestones invaded by seawater, acting as a barrier for the ascent of the liquid phase of geothermal fluids to the surface. Below, a conductive horizon interpreted as a clay cap approximately 1000 ± 500 meters thick overlies a less conductive horizon, which may correspond to a lateral fluid outflow zone rising from the deep reservoir and migrating along the regional fault network. This new conceptual model should be validated by exploration drilling to be carried out by Albioma Company. If successful, a geothermal power plant would be built for supplying electricity to Mayotte Island, reducing its dependence on fossil fuels.

1 INTRODUCTION

Mayotte is the oldest island of the Comoros Archipelago, estimated to be at least 26.5 Ma (Masquelet et al., 2022), which extends between the Mozambique and Madagascar (Figure 1.1). It is composed of Grande-Terre (363 km^2) and Petite-Terre (12 km^2). The island corresponds to an insular plateau structure of which only a small portion currently emerges above an ocean floor lying at approximately 3500 m depth. Mayotte is bordered by a coral barrier forming a lagoon, on which Petite-Terre is located. Petite-Terre Island has been investigated for its geothermal potential in the 2000's, notably due to two identified gas-emission areas: an intertidal zone in its southern part and Dziani crater lake (Figure 1.4). A campaign conducted by the French Geological Survey in 2005 (Traineau et al., 2006), including structural measurements, gas sampling, and geological fieldwork, led to a first conceptual model of the geothermal system. This conceptual model was focused on Petite-Terre Island and its recent volcanic activity. It is worth noting that, at the time and still today, no wells have been drilled. In 2018-2020, a sub-marine seismo-volcanic crisis near Mayotte revealed the existence of a submarine volcanic chain (the East Mayotte Volcanic Chain) through the eruption of the new Fani Maoré submarine volcano. This volcanic chain lies within a right-lateral transtensional corridor oriented N120–130° (Figure 1.2), related to the emerging boundary between the Lwandle and Somalia tectonic plates. Following the crisis, extensive offshore and onshore investigations provided unprecedented data on the subsurface. This paper integrates the new geological, geophysical, and geochemical data acquired during the crisis, to propose an updated conceptual model of the Petite-Terre geothermal system. The paper presents 1) the 2018–2020 seismo-volcanic crisis, 2) the geological context of the region, and then 3) the key results for geothermal exploration derived from the crisis, and 4) an updated conceptual model. These insights provide key information for guiding future geothermal exploration and drilling strategies on Petite-Terre.

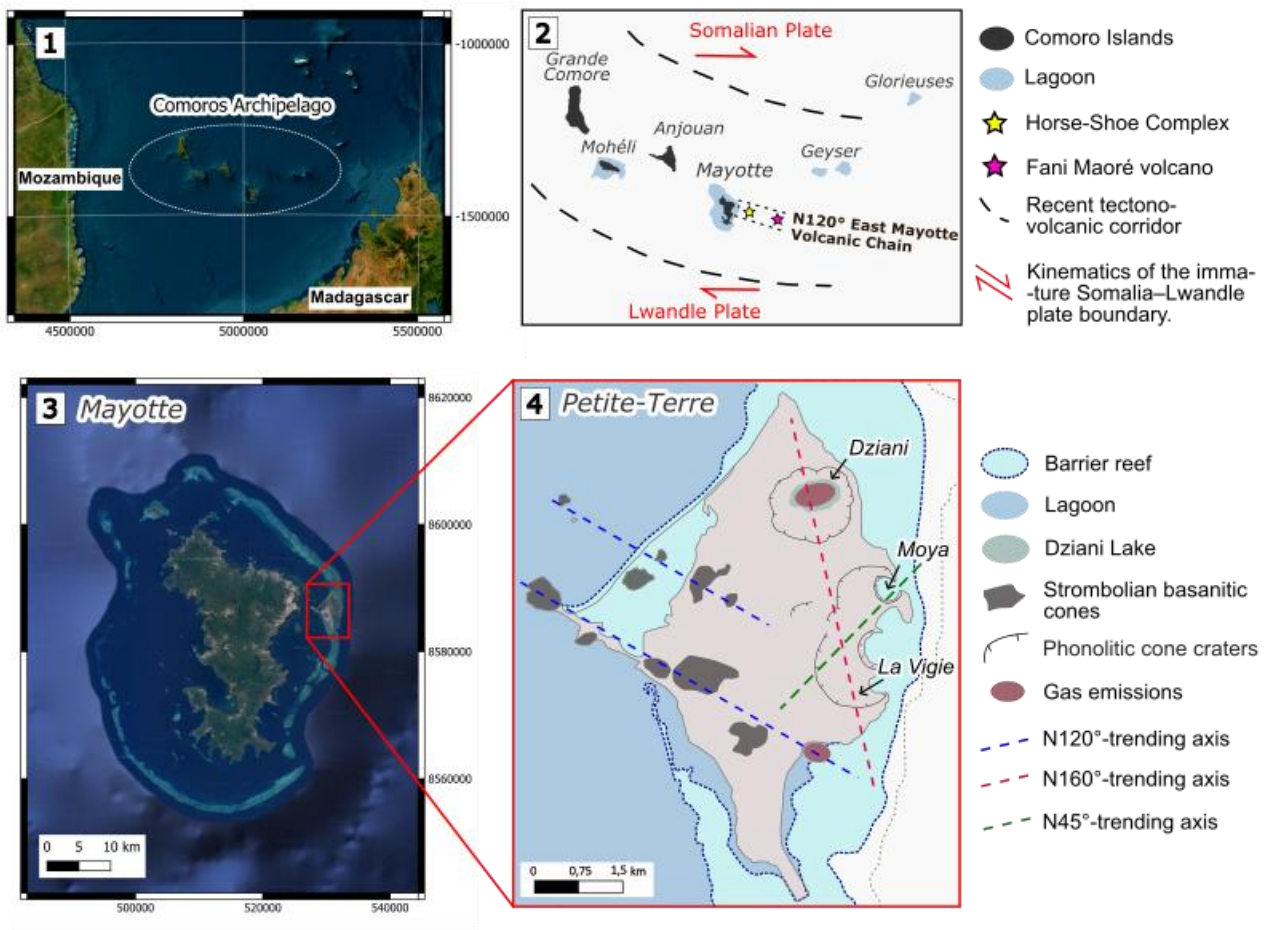


Figure 1 : 1) Geographical position of the Comoros Archipelago; 2) Simplified schematic of the archipelago showing the diffuse plate-boundary kinematics, with the Eastern Mayotte Volcanic Chain (EMVC); 3) Mayotte satellite imagery (EPSG:3857-WGS84/Pseudo-Mercator); 4) Interpretative schematic focused on Petite-Terre.

2 THE MAYOTTE 2018-2020 SEISMO-VOLCANIC CRISIS

2.1 Expression and characteristics of the crisis

A seismic crisis began in May 2018, about 50 km east of Mayotte, and was closely followed by a submarine eruption that formed the new volcanic edifice Fani Maoré (Figure 1.2). Between May and August 2018, seismic activity gradually migrated westward, 15–20 km offshore from Petite-Terre, near a complex volcanic structure known as the Horse-Shoe Complex (Figure 1.2). The distribution of seismicity highlighted two main clusters, with earthquakes occurring at about 30 km depth: a proximal cluster extending from Petite-Terre to the Horse-Shoe structure, and a distal cluster located 15 km farther offshore to the east. Seismicity has since remained concentrated in the proximal cluster, with Very Long Period (VLP) events typically associated with magmatic or hydrothermal fluid movements. Based on the earthquakes distribution, a magmatic system is located beneath the Horse-Shoe structure and likely comprises several magmatic reservoirs at varying depths between 50 to 20 km (Feuillet et al., 2021). Recent interpretations of MT survey beneath Mayotte also support the existence of deep magmatic reservoirs (Wawrzyniak et al, 2025). This magmatic system represents the source of the lavas that formed the new Fani Maoré volcano. Moreover, seismic data completed by bathymetric surveys, highlighted a N120–130°-oriented submarine volcanic chain east of Petite-Terre (Figure 1.2) including the Fani Maoré volcano, the Horse-Shoe Complex and recent phonolitic maars on Petite-Terre. Between July 2018 and late 2020, the volcanic crisis in Mayotte was expressed through ground deformation, with an eastward displacement of 21–25 cm and subsidence of 10–19 cm, consistent with the deflation of a deep source located east of the island (Lemoine et al., 2020; Feuillet et al., 2021; Peltier et al., 2022). In addition, changes in gas emissions were detected in the two areas of surface manifestations at Petite-Terre (Figure 1.4), as reflected in CO_2 fluxes, helium isotopic signatures, and equilibrium temperatures inferred from gas geothermometers.

2.2 Renewed scientific investigations and data acquisition

The 2018-2020 seismic crisis prompted renewed scientific interest leading to numerous coordinated offshore and onshore campaigns and research projects. These campaigns, including the MAYOBS missions and the REVOSIMA monitoring network, focused on characterizing underwater seismicity, mapping volcanic structures, and studying fluid emissions. Among these initiatives, the magnetotelluric (MT) method is of particular importance, as it is the most widely used geophysical technique for geothermal exploration in volcanic environments. In 2019 and 2021, the French Geological Survey (BRGM) conducted MT surveys, with IMAGIR consulting company supporting the analysis and 3D modelling of the acquired data. Both marine and onshore datasets were processed to produce a comprehensive 3D electrical resistivity model of Mayotte. As part of its Exclusive Exploration Permit on Petite-Terre, Albioma commissioned IMAGIR to refine the highest-resolution portion of the 3D resistivity model, covering the first five kilometers of depth beneath Petite-Terre. The MT results and their geological and geothermal interpretations are presented and discussed in section 4.3.

3 GEODYNAMIC AND GEOLOGICAL CONTEXTS

3.1 Geodynamic context, origin and structural inheritance of the Comoros Archipelago

From the Jurassic to the Early Cretaceous, the breakup of Gondwana was characterized by the formation of NE–SW oriented submarine ridges, which facilitated the opening of the Somalia and Mozambique basins, and the southward migration of Madagascar (Segoufin and Patriat, 1980; Coffin and Rabinowitz, 1987; Emmel et al., 2011; Mueller and Jokat, 2019). During the Cenozoic, the East African Rift System (EARS) developed and extended offshore from the Miocene to the Pliocene, forming several submarine grabens and major structural features such as the Davie Ridge (Chorowicz, 2005; Franke et al., 2015; Mcgregor, 2015). The Comoros Archipelago is now interpreted as a right-lateral tectono-volcanic corridor, representing an emerging boundary between the Somalia and Lwandle plates.

The Comoros archipelago exhibits a volcano-tectonic setting controlled both by regional tectonic inheritance and by local stress fields, the latter being inferred from the 2018-2020 seismo-volcanic crisis. At a large scale, the formation of the Comoros volcanic Islands and the location of volcanic edifices appear to be favored along N–S and N120–130° orientations, as observed at the recently formed Fani Maoré volcano. The N–S orientation corresponds to pre-existing structures inherited from Mesozoic tectonics (Davis et al., 2016), whereas the N120–130° trend is related to the emerging lithospheric plate boundary. A NE–SW orientation reflects regional faults associated with the East African Rift Zone (EARS) and faults in Madagascar (Tzevahirtzian et al., 2021). Finally, an E–W orientation is regionally expressed, particularly north of the Comoros archipelago, and mark the opening of the Somali Basin oceanic ridge (Stieltjes et al., 1988).

3.2 Geological setting of Mayotte and Petite-Terre Islands

Mayotte is the oldest island of the Comoros Archipelago, estimated to be at least 26.5 Ma. Volcanism evolved through multiple phases, with subaerial activity starting around 10 Ma (Debeuf, 2004; Nehlig et al., 2013). Around 0.75 Ma, a series of strombolian cones developed between the coral barrier (nowadays Petite-Terre Island) and Mayotte, aligned along an N120–130° trend (Figure 1.4). On Petite-Terre, these cones are intercalated within the coral barrier and were later covered by phreatomagmatic deposits from La Vigie, Moya and Dziani phonolitic maars, emplaced between 25 and 4 ka BP (Lacombe et al., 2024 and references therein) (Figure 1.4). The coral reef subsequently developed during the Pleistocene–Holocene and were exposed during the Last Glacial Maximum (≈ 26 ka BP), leading to their karstification. Based on Pajot et al. (2007) and Lacombe et al. (2024), the thickness of the coral barrier can be estimated at approximately 500–600 m. At the local scale on Petite-Terre, fractures have been mapped by Traineau et al. (2006) and Dezayes et al. (2023). Mapping reveals dominant NW–SE (N120–130°) orientation, with subordinate NNW–SSE (N160°) and NE–SW (N45°) trends. The NW–SE (N120–130°) trend at Petite-Terre corresponds to alignments of basanitic strombolian cones (blue dashed lines in Figure 1.4), likely representing subsurface dykes. The NNW–SSE (N160°) orientation is associated with alignment of phonolitic maars of Dziani, Moya, and La Vigie (red dashed lines in Figure 1.4). The NE–SW (N45°) trend is less common (green dashed lines in Figure 1.4) but represents the onshore projection of a submarine cones alignment observed northeast of Petite-Terre. Although fractures are clearly visible at outcrop scale on Petite-Terre, no major fault zone or significant tectonic structure has been identified.

3.3 Stress field and tectonic regime

The regional principal stress orientations, derived from focal mechanisms of earthquakes related to the 2018–2020 crisis (Famin et al., 2020), are as follows (dip/azimuth): σ1 (maximum horizontal stress) 14°/322°, σ2 (vertical stress) 59°/077°, and σ3 (minimum horizontal stress) 27°/224°. The stress field is consistent with a dextral transtensional tectonic regime along the diffuse boundary between the Somalia and Lwandle plates. This

indicates that the regional tectonic regime combines strike-slip motion with a normal component. The orientation of structures relative to the stress field strongly controls magma ascent pathways and, potentially, geothermal fluid circulation. Accordingly, the N120–130° structural trend (alignment of basanitic strombolian cones on Petite-Terre), parallel to the dextral transtensional shear (Figure 1.2), represents the most favorable pathways for fluid circulation. In contrast, the N45° structures, approximately perpendicular to the main shear, mainly accommodate lateral displacement and should be less effective as conduits for fluid circulation. The N160° structures corresponding to the phonolitic cones alignment on Petite-Terre Island, are oblique to the main stress direction, and may locally facilitate fluid migration under the normal component but are overall less efficient than the N120–130°-oriented structures. It should also be noted that intersections of volcano-tectonic structures can act as local controls on fluid circulation and are considered to be priority targets in geothermal system. These interpretative results, derived from magma pathways, are applied to the conceptual model of the geothermal system to propose pathways of geothermal fluid flow (section 5.3).

4 AVAILABLE DATA ON GEOTHERMAL RESOURCES OF PETITE-TERRE

4.1 Surface manifestations

Petite-Terre Island shows none of the usual surface indicators of a geothermal resource, such as thermo-mineral springs, warm soils, travertine deposits, or thermal anomalies in water wells and shallow aquifers (Traineau et al., 2006). Analyses of water samples collected in a water well onshore and within the intertidal gas emissions area reveal no evidence of contamination by deep geothermal fluids. However, it should be noted that the the seawater-saturated, karstified reef limestones, estimated to be 500–600 m thick (section 3.2), may act as an effective barrier to potential upward migration of geothermal fluids, at least in their liquid phase. The hypothesis is that geothermal fluids could be diluted within the very large volume of seawater. The only surface hydrothermal manifestations on Petite-Terre are persistent gas emissions at two locations: within the Dziani crater lake and in an intertidal zone (dark pink in Figure 1.4). Figure 2 (left) presents a view of the Dziani crater lake showing two areas of gas emissions, highlighted by white foam as observed in July 2025. Gas emissions in Dziani crater lake have long been known. However, their intensity increased during the 2018–2020 seismic-volcanic crisis and has remained high since. The two surface bubbling areas of the lake were each estimated to cover at least 500 m^2.



Figure 2 : Left : View of Dziani crater lake showing two gas emissions areas highlighted by white foam (July 2025). Right : Close view of gas bubbles escaping from small cavities in Petite-Terre's intertidal zone (Traineau et al., 2006). The locations are shown on the map in Figure 1.4.

Figure 2 (right) shows the intertidal zone where gas emissions occur. Gas bubbles escape from small cavities in the sand, forming numerous chains of bubbles in the water at high tide. In 2005 and 2008, the bubbling area was estimated to be 250 m x 300 m, with more than 2,000 gas exit points recorded (Traineau et al., 2006; Sanjuan et al, 2008). No chemical or thermal anomaly were measured in the seawater. On the other hand, seawater pH, which is usually in the range of 8.1-8.2, was around 5.8 near the most important gas vents, likely due to CO_2 dissolution. Sanjuan et al. (2008) measured a gas flux of 16 L/min at the main vent and estimated the daily gas flux at 0.31 kg/day/m^2.

4.2 Gas geochemistry

The gases collected at Petite-Terre Island are composed of approximately 98% CO_2, 0.2% CH_4, and contain a relatively high helium concentration along with trace amounts of radon (Sanjuan et al., 2008). The $\delta^{13}C$ measured on the CO_2, $^3He/^4He$ isotopic ratios, and neon isotopes indicate a deep mantle origin (Sanjuan et al., 2008). During the seismo-volcanic crisis, monitoring systems were implemented to track changes in gas emissions. CO_2 emissions increased during the seismic crisis, then gradually decreased and have now stabilized (REVOSIMA bulletin). Changes such as a gradual decrease in pH, a sharp drop in dissolved inorganic carbon,

and an increase in the normalized $^{3}He/^{4}He$ ratio were also measured. The equilibrium temperatures inferred from the CO_2/CH_4 isotopic geothermometer also change. At the intertidal zone, it decreased from 330°c to 290°C between 2020 and 2023, while gases emitted at Dziani crater lake had equilibrium temperature increasing from 230°C to 260° (REVOSIMA Bulletin). In addition, large acoustic plumes associated with gas presence have been detected in the seawater column above the Horse-Shoe volcanic complex while some sites on sea bottom floor exhibiting liquid CO_2 degassing. The elemental and isotopic signatures of gases emitted at the Horse-Shoe complex are similar to those observed onshore at Petite-Terre (REVOSIMA Bulletin). As the gas emissions observed in the intertidal zone near La Vigie and within Dziani crater lake were affected by the seismo-volcanic crisis, their origin can be linked to the activity of the Horse-Shoe volcanic complex. The N120–130° volcano-tectonic structures, which has controlled the emplacement of the basanitic strombolian cones on Petite-Terre as well as the submarine volcanic edifices extending to the Horse-Shoe complex, are supposed to control gas (and geothermal fluid) circulations toward Petite-Terre. Therefore, the N120–130° structures will represent priority targets for exploration of the Petite-Terre geothermal resources.

4.3 3D electrical resistivity distribution

As described in section 2.2, IMAGIR (2025) reprocessed the highest-resolution 3D electrical resistivity model down to 5 km depth beneath Petite-Terre. Fourteen onshore MT soundings on Petite-Terre and eighteen offshore soundings (legend below Figure 3) were acquired in 2019 and 2021 by BRGM, using Metronix and STATEM/MAPPEM Geophysics instruments, respectively.

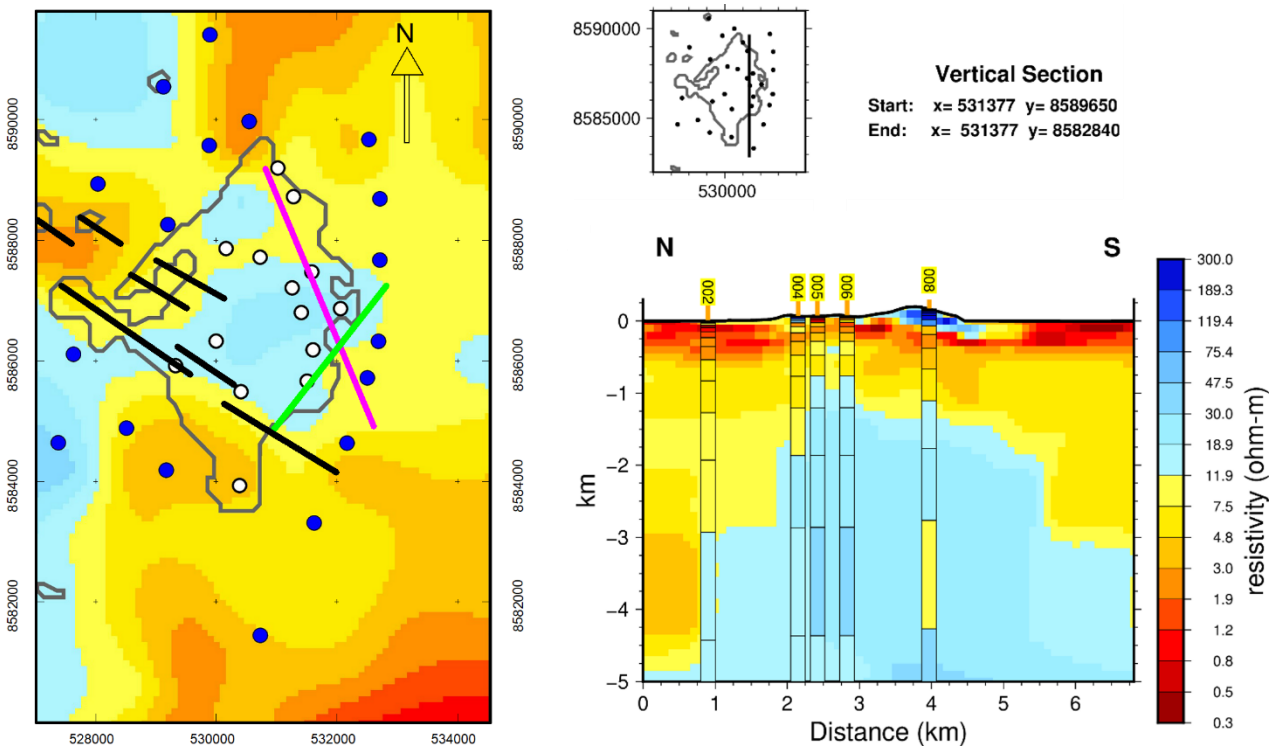


Figure 3 : Left: Resistivity distribution map at 1500 m depth; Right: N–S cross-section showing the resistivity distribution (IMAGIR, 2025 ; based on data acquired by BRGM). White dots: onshore MT soundings; Blue dots : offshore MT soundings; Black line: basanitic cones alignments; Pink line: phonolitic cones alignment; Green line: submarine cones alignment projected onshore.

Two grids were created: a computation grid for numerical accuracy, and an inversion grid, which was adapted to the data resolution. The former depends on the spatial distribution of MT soundings, while the latter varies with depth and distance from the sites. A 3D inversion was then performed by IMAGIR to derive the resistivity distribution that best reproduces the observed MT impedances. All details on MT data processing and 3D inversion methods are described in Wawrzyniak et al. (2025). Extracted map and sections from the 3D model that are most relevant are shown here (Figure 3 and Figure 4) : the resistivity map at 1500 m depth, a N–S-oriented cross-section in the eastern part of Petite-Terre and a W-E-oriented cross-section across the central part of Petite-Terre. The 3D modeling of MT data by IMAGIR (2025) highlights several observations:

- A very conductive near-surface horizon (0–5 ohm·m) with a thickness of 400–500 m, likely corresponding to reef limestones of the coral barrier, possibly karstified and seawater-invaded;

- A low-resistivity horizon (5–12 ohm·m) interpreted as a clay cap (smectite zone), with a thickness of 1000 ± 500 m. Doming structures at the base of the clay cap as seen on Figure 3 may indicate upward circulation of geothermal fluids, particularly along inferred tectonic structures/dykes;

- A deeper horizon with slightly higher resistivity (12–50 ohm·m), interpreted as a potential geothermal reservoir.

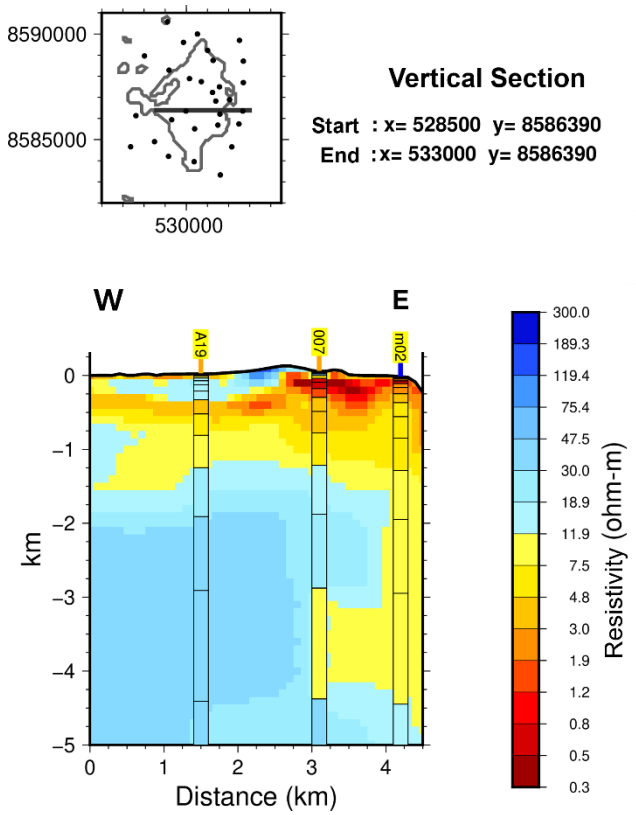


Figure 4 : W–E cross-section showing the resistivity distribution in the central part of Petite-Terre Island (IMAGIR, 2025 ; based on data acquired by BRGM).

The resistivity distribution at depth beneath Petite-Terre Island is consistent with the presence of a high temperature geothermal reservoir. Changes in gas emissions observed during the seismo-volcanic crisis could support the presence of an active geothermal system and discard the hypothesis of a fossil system. By analogy with well-known high temperature geothermal reservoirs, temperatures at the bottom of the clay-cap might be around 180°C (Anderson et al., 2000).

5 DISCUSSION AND INTERPRETATION : DEVELOPMENT OF THE CONCEPTUAL MODEL

5.1 Potential heat source

Following BRGM's 2006 exploration survey, the geothermal system was initially thought to derive its heat from recent volcanic activity expressed by the phonolitic maars of Dziani and La Vigie-Moya. The 2018–2020 seismo-volcanic crisis provided new insights, including ground deformation on Petite-Terre, increased gas emissions in Dziani crater lake and in an intertidal zone, and changes in gas composition. These observations demonstrate that Petite-Terre is thermally and structurally connected to the offshore Horse-Shoe volcanic complex where a persistent volcanic activity, gas emissions and seismic cluster have been recorded. Deep volcano-tectonic (VT) and shallower very-low-frequency (VLF) earthquakes indicate the presence of magmatic chambers near the Moho and deeper, at approximately 20-50 km depth beneath the Horse-Shoe complex. The 3D MT inversion results also support the presence of magmatic reservoirs (Wawrziniak et al., 2025). These deep magmatic chambers fed the eruptions of the new Fani Maoré volcano through lateral magma migration oriented along N120–130°, and most likely the older volcanic cones, aligned along the same trend on Petite-Terre. High temperature magmatic fluids from magma degassing are considered as the heat source of the Petite-Terre geothermal system (see Figure 5 below).

5.2 New conceptual reservoir model

Figure 5 presents a NW–SE-oriented cross-section (1:1 scale) of the proposed conceptual reservoir model. This section provides a synthetic view of the different components of the model: the heat source, deep volcano-tectonic structures, magmatic gas pathways, seawater infiltration, the deep geothermal reservoir, geothermal fluid circulation, and the clay-rich cap. Deep magmatic fluids are inferred to rise vertically beneath the Horse-Shoe caldera structure proposed by Feuillet et al. (2021) from a magmatic reservoir located at approximately 20 km depth as deduced from the distribution of VT and VLF earthquakes. The Horse-Shoe caldera is assumed to be the preferential site of seawater infiltration also. Mixing between ascending high-temperature magmatic fluids and descending seawater is thought to take place within this caldera structure somewhere between 2 and 5 km depth below the seafloor. This mixing zone would constitute the deep geothermal reservoir, where the geothermal fluid would equilibrate chemically and thermally at 250–300 °C, according to the CO_2/CH_4 gas geothermometer. The lateral extent of this deep reservoir would correspond to a “lateral outflow” from the caldera structure along extensional fault and dyke networks oriented N120–130°.

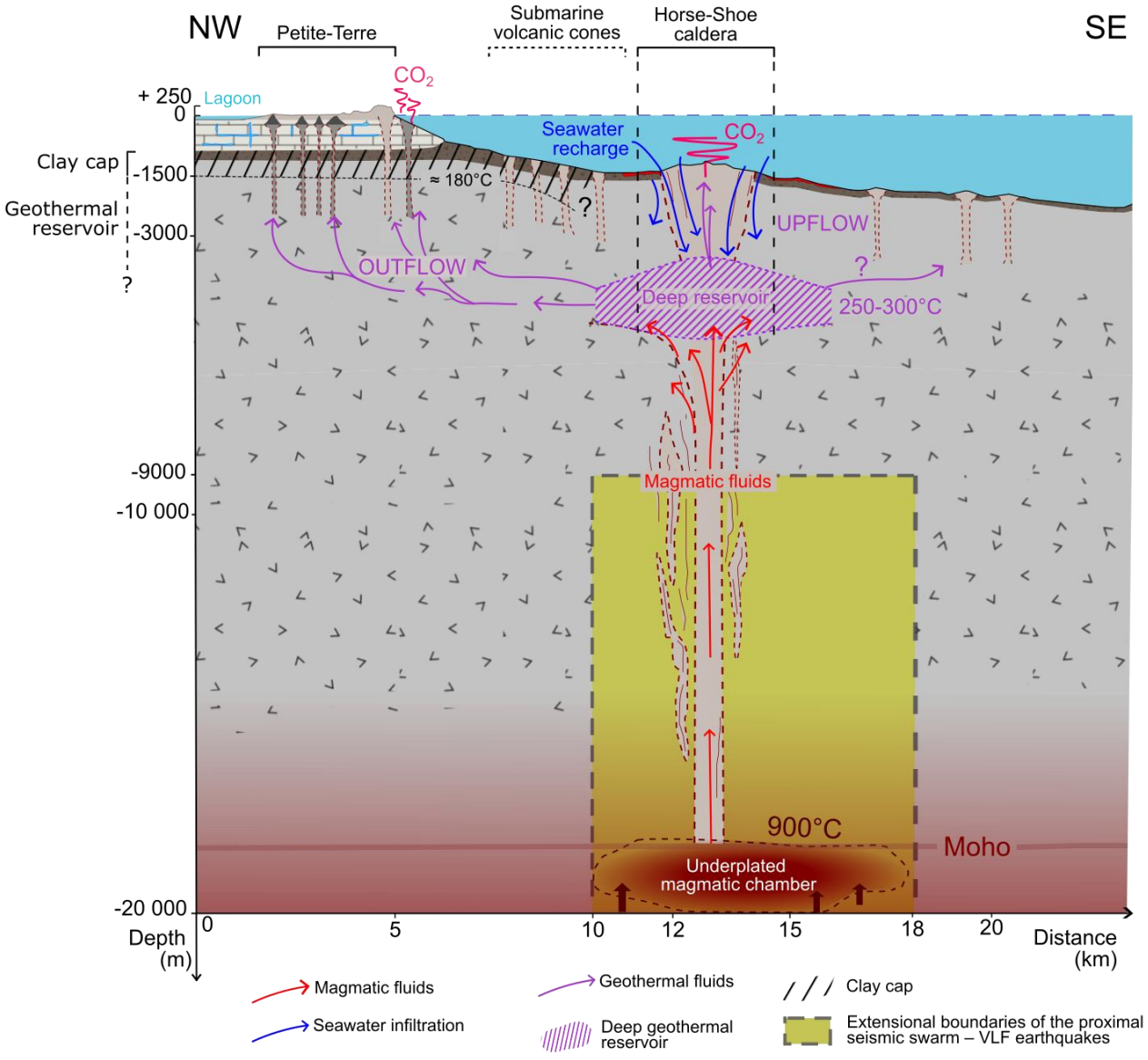


Figure 5 : New conceptual model of the Petite-Terre high-temperature geothermal reservoir, illustrated as a 1:1 scale cross-section oriented N120–130°.

5.3 Fluids circulation pathways

The proposed conceptual model suggests that the deep geothermal reservoir is not located directly beneath Petite-Terre Island but is laterally offset, associated with the submarine Horse-Shoe volcanic complex, located 10–15 km to the southeast. The geothermal fluid is supposed to be seawater with its chemical composition likely modified through interactions with the host rock and magmatic gases. By analogy with other geothermal systems

dominated by seawater recharge, such as the Reykjanes field in Iceland, the mineral phases expected to precipitate include silica, calcite, anhydrite, polymetallic sulfides, and NaCl salt (Arnórsson, 1978; Sveinbjörnsdóttir et al., 1986).

The upflow zone above the deep reservoir is evidenced by gas emissions observed at the seafloor within and near the caldera structure (Figure 5). Lateral fluid outflow is thought to develop from the deep reservoir towards Petite-Terre, primarily along the N120–130°-oriented fault and dyke networks, representing the most favorable pathways (see section 3.3). Gas emissions observed in the intertidal zone and in Dziani crater lake are interpreted as evidence of this lateral fluid flow pattern. The development of long-distance lateral fluid outflow zones from deep geothermal reservoirs has been documented in several exploited geothermal fields (Henley and Ellis, 1983; Molina and Marti, 2016; Simpson and Bignall, 2016; Stimac et al., 2019; Pratama et al., 2024). This interpretation is further supported by the resistivity distribution, which shows a pattern consistent with a clay cap overlying a reservoir (Figure 3 and Figure 4). Dome-shaped resistivity geometries at the base of the inferred clay cap support the hypothesis of geothermal fluid circulations, at depth that could be targeted by drilling.

5.4 Temperature and pressure prognostics

With no wells drilled, the only available indicator for estimating the temperature of the deep geothermal reservoir is provided by CO_2/CH_4 gas geothermometer, which indicates an equilibrium temperature of around 250–300°C (REVOSIMA bulletin). This temperature value is therefore considered representative of conditions within the deep reservoir. Beneath Petite-Terre Island, the temperature of the geothermal fluid is expected to be slightly lower than that of the deep reservoir due to cooling during its travel. In wells, thermal inversions are expected in the temperature profiles, with a maximum temperature observed when intersecting the permeable zones. The expected pressure within the geothermal reservoir corresponds to the hydrostatic pressure of a seawater column, corrected for temperature effects on fluid density.

5.5 Age of the Petite-Terre geothermal system

The heat source of the geothermal system is likely related to magmatic activity of the Horse-Shoe submarine volcanic complex. The age of this submarine volcanic complex is not yet determined. However, the numerous volcanic structures identified within the Horse-Shoe area suggest a long-lived submarine volcanic activity. Dredged samples from the Horse-Shoe complex reveal phonolitic lavas with petrographic characteristics similar to those of the phonolitic maars of Petite-Terre (Dziani, La Vigie, and Moya). The latter are not dated but supposed to be few thousand to few ten thousand years old. The sustained volcanic activity over such timescales is favorable to the development of a deep high-temperature geothermal reservoir. Nevertheless, in the absence of subsurface data, the current maturity of the geothermal system remains difficult to evaluate.

6 CONCLUSION

The 2018–2020 sub-marine seismo-volcanic crisis East of Mayotte Island greatly improves the understanding of the two gas emission areas recorded in Petite-Terre Island during the 2005 geothermal exploration campaign in terms of potential geothermal resources. One of the major outcomes was the discovery of a submarine volcanic chain (the Eastern Mayotte Volcanic Chain) to the East of Petite-Terre and oriented N120-130°. Basanitic strombolian cones on Petite-Terre are aligned along the same N120–130° trend. This structural orientation corresponds to the regional extensional stress field that favors the opening of tectonic structures and dykes, and enhances the permeability needed for magma ascent and geothermal fluid circulations. The recent phonolitic maars of Dziani, Moya and La Vigie are now related to this volcanic chain.

Another major outcome was the evidence of the sub-marine Horse-Shoe volcanic complex located around 10 km from Petite-Terre Island. This volcanic complex was a main locus of earthquakes and the deep source of magma emitted during the eruption of the new Fani Maoré volcano. It is also the site of CO_2 liquid emissions at the sea floor which are similar to the gas emissions observed in the intertidal zone and the Dziani crater lake on Petite-Terre Island. The latter showed some changes during the seismo-volcanic crisis. The amount of gas emissions increased and the chemical and isotopic compositions of gas ($^3He/^4He$ ratio or the CO_2/CH_4 isotopic geothermometer) also evolved. It is viewed as evidence of connections between the Horse-Shoe volcanic complex and these surface hydrothermal manifestations along N120–130° volcano-tectonic structures.

This work proposes a novel conceptual model of the Petite-Terre high-temperature geothermal system, placing the deep reservoir offshore beneath a coral reef. These outcomes support a revised interpretation in which the heat source and deep geothermal reservoir are not located beneath Petite-Terre Island but are laterally shifted eastward beneath the Horse-Shoe volcanic complex. Reservoir temperatures are estimated to range between

250 and 300°C based on gas isotopic geothermometry. Consequently, lateral fluid outflows are expected beneath Petite-Terre Island, with temperatures likely lower than those of the deep reservoir. This interpretation is consistent with the resistivity distribution derived from magnetotelluric soundings. It should be noted that the presence of the geothermal system and its current activity state remain to be confirmed by exploratory drilling. To conclude, this new conceptual model of Petite-Terre's geothermal system provides a basis for planning exploration strategies and designing the first geothermal exploration wells. The forthcoming drilling campaign, planned over the next three years, will provide confirmation of the geothermal system beneath Petite-Terre.

Acknowledgements

We acknowledge the Conseil Départemental of Mayotte and BRGM for their permission to use the resistivity data acquired from magnetotelluric soundings.

REFERENCES

Anderson, E., Crosby, D., Ussher, G.: Bulls-eye! Simple resistivity imaging to reliably locate the geothermal reservoir. In *Proceedings World Geothermal Congress*, (2000, May), 909-914.

Arnórsson, S.: Major element chemistry of the geothermal sea-water at Reykjanes and Svartsengi, Iceland, *Mineralogical Magazine*, **322**, (1978), 209-220.

Chorowicz, J.: The East African rift system, *J. Afr. Earth Sci.*, **1–3**, (2005), 379–410.

Coffin, M.F., Rabinowitz, P.D.: Reconstruction of Madagascar and Africa: evidence from the Davie fracture zone and western Somali basin, *J. Geophys. Res. Solid Earth Planets*, **B9**, (1987), 9385–9406.

Davis, J.K., Lawver, L.A., Norton, I.O., Gahagan, L.M.: New Somali Basin magnetic anomalies and a plate model for the early Indian Ocean, *Gondwana research*, (2016), 16-28.

Debeuf, D.: Étude de l'évolution volcano-structurale et magmatique de Mayotte (archipel des Comores, océan Indien), *Doctoral Dissertation*, *Université de la Reunion*, (2004).

Dezayes, C., Stopin, A., Wawrzyniak, P., Gal, F., Farlotti, T., Armandine Les Landes, A., Calcagno, P., Traineau, H., Hirsinger, L., Macedo Serrano, E., Chassagne, R.: Exploration des potentielles ressources géothermiques profondes de Petite Terre (Mayotte), *rapport final BRGM/RP-72283-FR*, (2023).

Emmel, B., Kumar, R., Ueda, K., Jacobs, J., Daszinnies, M.C., Thomas, R.J., Matola, R.: Thermochronological history of an orogen-passive margin system: an example from northern Mozambique, *Tectonics*, **2**, (2011).

Feuillet, N., Jorry, S., Crawford, W.C., Deplus, C., Thinon, I., Jacques, E., Saurel, J.M., Lemoine, A., Paquet, F., Satriano, C., Aiken, C., Foix, O., Kowalski, P., Laurent, A., Rinnert, E., Cathalot, C., Donval, J.P., Guyader, V., Gaillot, A., Scalabrin, C., Moreira, M., Peltier, A., Beauducel, F., Grandin, R., Ballu, V., Daniel, R., Pelleau, P., Gomez, J., Besançon, S., Geli, L., Bernard, P., Bachelery, P., Fouquet, Y., Bertil, D., Lemarchand, A., Van der Woerd, J.: Birth of a large volcanic edifice offshore Mayotte via lithosphere-scale dyke intrusion, *Nature Geoscience*, **10**, (2021), 787-795.

Franke, D., Jokat, W., Ladage, S., Stollhofen, H., Klimke, J., Lutz, R., Mahanjane, E.V., Ehrhardt, A., Schreckenberger, B.: The offshore East African Rift System: Structural framework at the toe of a juvenile rift, *Tectonics*, **10**, (2015), 2086-2104.

Henley, R.W., and Ellis, A.J.: Geothermal systems ancient and modern: A geochemical review, *Earth Science Review*, (1983), 1-50.

Lacombe, T., Gurioli, L., Di Muro, A., Médard, E., Berthod, C., Bachèlery, P., Bernard, J., Sadeski, L., Komorowski, J. C.: Late Quaternary explosive phonolitic volcanism of Petite-Terre (Mayotte, Western Indian Ocean), *Bulletin of Volcanology*, **2**, (2024).

Lemoine, A., Briole, P., Bertil, D., Roullé, A., Foumelis, M., Thinon, I., Raucoules, D., De Michele, M., Valty, P., Hoste Colomer, R.: The 2018–2019 seismo-volcanic crisis east of Mayotte, Comoros islands: seismicity and ground deformation markers of an exceptional submarine eruption, *Geophys. J. Int.*, **1**, (2020), 22–44.

McGregor, D.: History of the development of the East African Rift system: a series of interpreted maps through time, *J. Afr. Earth Sci.*, (2015), 232–252.

Masquelet, C., Leroy, S., Delescluse, M., Chamot-Rooke, N., Thinon, I., Lemoine, A., Franke, D., Watremez, L., Werner, P., Paquet, F., Berthod, C., Cabiativa, V., Sauter, D. : Le nouveau volcan de l'Est-Mayotte dans l'archipel des Comores: structure et chronologie des phases magmatiques déduites des données d'imagerie sismique, *Comptes Rendus Geoscience*, **2S**, (2022), 65-79.

Molina, F., and Marti, J.: The Borinquen geothermal system (Canas Dulce, Costa Rica), *Geothermics*, (2016), 410-425.

Mueller, C.O., and Jokat, W.: The initial Gondwana break-up; a synthesis based on new potential field data of the Africa-Antarctica corridor, *Tectonophysics*, (2019), 301–328.

Nehlig, P., Lacquement, F., Bernard, J., Audru, J.-C., Caroff, M., Deparis, P., Jaouen, T., Pelleter, A.-A., Perrin, J., Prognon, C., Vittecoq, B. : Notice explicative, Carte géol. France (1/30 000), feuille Mayotte (1179), *BRGM*, (2013)

Pajot, G., Debeglia, N., Miehé, J.-M.: Estimation du potentiel géothermique de Mayotte : Phase 2 – Etape 1. Investigations géophysiques par gravimétrie, magnétisme et panneau de résistivité électrique, *Rapport Intermédiaire BRGM/RP-56027-FR*, (2007).

Peltier, A., Saur, S., Ballu, V., Beauducel, F., Briole, P., Chanard, K., Daussed, D., De Chabaliera, J.-B., Grandin, R., Rouffiac, P., Tranchant, Y.-T., Bès de Berc, M., Besançon, S., Boissier, P., Broucke, C., Brunet, C., Canjamalé, K., Carme, E., Catherine, P., Colombain, A., Crawford, W., Daniel, R., Dectot, G., Desfete, N., Doubre, C., Dumouch, T., Griot, C., Grunberg, M., Jund, H., Kowalski, P., Lauret, F., Lebreton, L., Pesqueira, F., Tronel, F., Valty, P., Van Der Woerd, J.: Ground deformation monitoring of the eruption offshore Mayotte, *Comptes Rendus Géoscience*, **S2**, (2022), 1-23.

Pratama, H.B., Katsuaki, K., Pratama, A.B., Ashat, A.: Model of a post-caldera volcano-hosted and vapor-dominated system through a numerical simulation study of the Bedugul geothermal field, Bali Island, Indonesia, *Geothermics*, (2024).

Sanjuan, B., Baltassat, J.-M., Bezelgues, S., Brach, M., Girard, J.-F., Mathieu, F. : Estimation du potentiel géothermique de Mayotte : Phase 2 - Etape 2. Investigations géologiques, géochimiques et géophysiques complémentaires, synthèse des résultats, *BRGM/RP-56802-FR*, (2008).

Segoufin, J., Patriat, P.: Existence d'anomalies mésozoïques dans le bassin de Somalie. Implications pour les relations Afrique-Antarctique-Madagascar, *Comptes Rendus de l'Académie des Sciences,* **1980**, (1980), 85–88.

Simpson, M.P., and Bignall, G.: Undeveloped high-enthalpy geothermal field of the Taupo Volcanic Zone, New Zealand, *Geothermics*, (2016), 325-346.

Stimac J., Ganefianto, N., Baroek, M., Sihotang, M., Ramadhan, I., Mussofan, W., Sidik, R., Alfiady, Dyaksa, D.A., Azis, H., Putra, A.P., Martikno, R., Irsamukhti, R., Santana, S., Matsuda, K., Hatanaka, H., Soeda, Y., Cariou, L., Egermann, P.: An overview of the Muara Laboh geothermal system, Sumatra, *Geothermics*, (2019), 150-167.

Stieltjes, L.: Carte géologique de Mayotte au 1/50 000 et sa notice explicative, *Editions du BRGM*, (1988).

Sveinbjornsdottir, A.E., Coleman, M.L., Yardley, B.W.D.: Origin and history of hydrothermal fluids of the Reykjanes and Krafla geothermal fields, Iceland: A stable isotope study, Contributions to *Mineralogy and Petrology*, (1986), 99-109.

Tzevahirtzian, A., Zaragosi, S., Bachèlery, P., Biscara, L., Marchès, E.: Submarine morphology of the Comoros volcanic archipelago, *Marine Geology*, (2021).

Thinon, I., Lemoine, A., Leroy, S., Paquet, F., Berthod, C., Zaragosi, S., Famin, V., Feuillet, N., Bloymond, P., Masquelet, C., Mercury, N., Rusquet, A., Scalabrin, C., Van der Woerd, J., Bernard, J., Bignon, J., Clouard, V., Doubre, C., Jacques, E., Jorry, S.J., Rolandone, F., Chamot-Rooke, N., Delescluse, M., Franke, D., Watremez, L., Bachèlery, P., Michon, L., Sauter, D., Bujan, S., Canva, A., Dassie, E., Roche, V., Ali, S., Sitti Allaouia, A. H., Deplus, C., Rad, S., Sadeski, L.: Volcanism and tectonics unveiled in the Comoros Archipelago between Africa and Madagascar, *Comptes Rendus Géoscience*, **S2**, (2022), 7-34.

Traineau, H., Sanjuan, B., Brach, M., Audru, J.-C.: Etat des connaissances du potentiel géothermique de Mayotte, *BRGM/RP-54700-FR*, (2006).

Wawrzyniak, P., Gaillard, F., Hautot, S., Andujar, J., Tarits, P., Arbaret, L., Guegan, S., Sifré, D., D'Eu, J-F., Deparis, J., Lemoine, A., Thinon, T., Warden, S., Dubois, F.: Magnetotelluric evidence for a melt-rich magmatic reservoir beneath Mayotte, *Nature*, (2025), 1122-1128.